

BIAS REDUCTION FOR THE SCAN-BASED LEAST-SQUARES EMITTER LOCALIZATION ALGORITHM

Kutluyıl Doğançay and Samuel P. Drake

School of Electrical & Information Engineering
University of South Australia
Mawson Lakes, SA 5095, Australia
Email: kutluyil.dogancay@unisa.edu.au

Electronic Warfare and Radar Division
Defence Science and Technology Organisation
Edinburgh, SA 5111, Australia
Email: sam.drake@dsto.defence.gov.au

ABSTRACT

This paper presents bias reduction techniques for the scan-based least-squares emitter localization algorithm. Scan-based emitter localization exploits constant scan rate of the radar antenna main beam to allow determination of the emitter location by three or more receivers. It does away with high-precision timing requirements for time of arrival measurements for intercepted radar beams and does not require high-sensitivity receivers to pick up sidelobes of the radar beam pattern. The paper develops a weighted least-squares estimator and an iterative maximum likelihood estimator to overcome the least-squares estimation bias. The improved bias performance is illustrated with simulation examples.

1. INTRODUCTION

Passive emitter localization is an important research problem with many civilian and military applications including user location in wireless mobile communication systems, and target location and tracking in electronic warfare systems.

Several techniques are available for passive location of an emitter, each with certain advantages and disadvantages. This makes the identification of a single best localization approach for all applications very difficult. As a result the localization research has mainly focused on the development of high-performance techniques tailored for particular applications. Most passive localization techniques utilize angle-of-arrival (bearings), Doppler shift, time of arrival, time difference of arrival, and received signal energy measurements. Hybrid approaches employing a combination of these are also available. A critique of time difference of arrival techniques, which are well suited to locating uncooperative emitters, is the requirement of high-precision time of arrival measurements and highly synchronized clocks at multiple receivers. The receivers are also assumed to be capable of picking up the same emitted signal at different locations. The scan-based localization technique was recently proposed to do away with some of these difficulties for locating a particular type of radar, viz., pulsed radar with constant rotation-speed antenna beam [1]. The scan-based localization technique is closely related to rotating directional beacon techniques presented in [2, 3].

This paper presents bias reduction techniques for the scan-based least-squares emitter localization algorithm. Two new algorithms are developed for multiple scan measurements; viz., weighted least squares algorithm

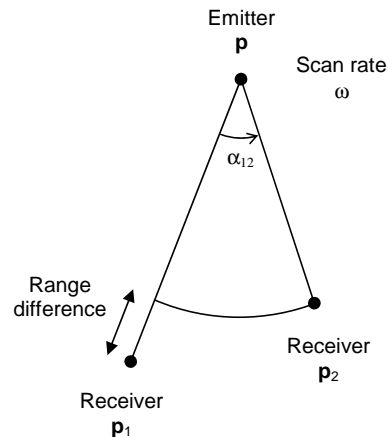


Figure 1: The subtended angle α_{12} depends on the scan rate ω and arrival times of the radar pulses at the receivers. Throughout this report the time delay due to range difference is ignored.

and maximum likelihood estimator. The performance improvement achieved by these algorithms is illustrated with several simulation examples. The paper is organized as follows. The scan-based emitter localization algorithm is described in Section 2. The noise effects are studied in Section 3. In Section 4 the case of four or more receivers is considered and the linear least squares algorithm is developed. The maximum likelihood estimator is presented in Section 5. Section 7 presents comparative simulation studies.

2. SCAN BASED EMITTER LOCALIZATION ALGORITHM

The scan based emitter localization algorithm [1] exploits constant scan rate of the radar antenna main beam. Assuming that the scan rate (angular velocity) ω is known or estimated, it uses the pulse arrival times at multiple receivers as the radar beam sweeps across them (see Fig. 1). Given a pair of receivers at known locations p_1 and p_2 , the subtended angle is given by

$$\alpha_{12} = \omega |t_2 - t_1| \quad (1)$$

where t_1 and t_2 are the time of arrival (TOA) measurements for the centroid of the main lobe of the radar beam at receivers p_1 and p_2 . Here the additional time delay due to range difference between the two receivers

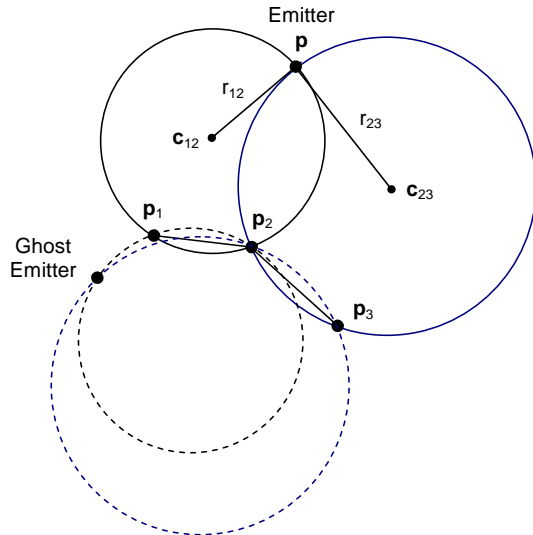


Figure 2: Scan-based emitter localization using three receivers. The ghost emitter may be eliminated by making use of directional information or prior knowledge of direction of rotation for the emitter.

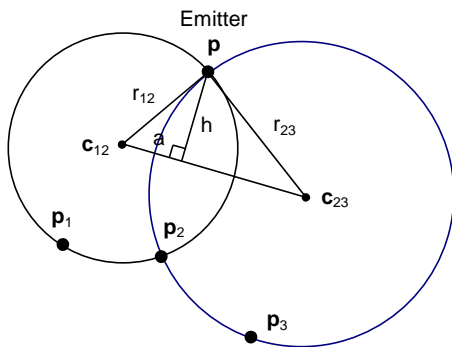


Figure 3: Closed-form solution to the emitter location.

is neglected since it is usually quite small compared with the time it takes for the beam to sweep across from one receiver to another. Given α_{12} and the receiver locations \mathbf{p}_1 and \mathbf{p}_2 , the loci of all possible locations for the emitter form a circular arc with centre point \mathbf{c}_{12} and radius r_{12} :

$$\mathbf{c}_{12}^{\pm} = \frac{\mathbf{p}_1 + \mathbf{p}_2}{2} + \mathbf{R}_{12}^{\pm\pi/2} \frac{\mathbf{p}_2 - \mathbf{p}_1}{2 \tan \alpha_{12}}, \quad r_{12} = \frac{\|\mathbf{p}_2 - \mathbf{p}_1\|_2}{2 \sin \alpha_{12}} \quad (2)$$

where $\|\cdot\|_2$ denotes the Euclidean norm and $\mathbf{R}_{12}^{\pm\pi/2}$ is the $\pm 90^\circ$ rotation matrix

$$\mathbf{R}_{12}^{\pm\pi/2} = \begin{bmatrix} 0 & \mp 1 \\ \pm 1 & 0 \end{bmatrix}. \quad (3)$$

Only one of the circle centres \mathbf{c}_{12}^{\pm} corresponds to the true emitter location. The true circle centre can be determined from additional information such as direction of arrival. Denote the true circle centre by \mathbf{c}_{12} .

Consider now the scenario of three receivers at locations \mathbf{p}_1 , \mathbf{p}_2 and \mathbf{p}_3 (see Fig. 2). The emitter location \mathbf{p}

can be obtained from the following nonlinear equations

$$\|\mathbf{p} - \mathbf{c}_{12}\|_2 = r_{12} \quad (4a)$$

$$\|\mathbf{p} - \mathbf{c}_{23}\|_2 = r_{23}. \quad (4b)$$

A closed-form geometric solution to the emitter location can be formulated by considering the triangle formed by the circle centres and the emitter location (Fig. 3):

$$a = \frac{r_{12}^2 - r_{23}^2 + \|\mathbf{c}_{23} - \mathbf{c}_{12}\|_2^2}{2\|\mathbf{c}_{23} - \mathbf{c}_{12}\|_2} \quad (5a)$$

$$h = \sqrt{r_{12}^2 - a^2} \quad (5b)$$

$$\mathbf{u} = \frac{\mathbf{c}_{23} - \mathbf{c}_{12}}{\|\mathbf{c}_{23} - \mathbf{c}_{12}\|_2} \quad (5c)$$

$$\phi = \tan^{-1} \frac{h}{a} \quad (5d)$$

$$\mathbf{R}^{\pm\phi} = \begin{bmatrix} \cos \phi & \mp \sin \phi \\ \pm \sin \phi & \cos \phi \end{bmatrix} \quad (5e)$$

$$\mathbf{p} = \mathbf{c}_{12} + r_{12} \mathbf{R}^{\pm\phi} \mathbf{u} \quad (5f)$$

where $\mathbf{R}^{\pm\phi}$ is the $\pm\phi$ rotation matrix, which gives two possible solutions for \mathbf{p} . One of these solutions is \mathbf{p}_2 which can easily be eliminated.

Equation (4) can be linearized by taking the square of both sides of the equations:

$$\|\mathbf{p} - \mathbf{c}_{12}\|_2^2 = r_{12}^2 \quad (6a)$$

$$\|\mathbf{p} - \mathbf{c}_{23}\|_2^2 = r_{23}^2. \quad (6b)$$

Subtracting the second equation from the first one gives

$$\|\mathbf{p} - \mathbf{c}_{12}\|_2^2 - \|\mathbf{p} - \mathbf{c}_{23}\|_2^2 = r_{12}^2 - r_{23}^2 \quad (7a)$$

$$(\mathbf{p} - \mathbf{c}_{12} - \mathbf{p} + \mathbf{c}_{23})^T (\mathbf{p} - \mathbf{c}_{12} + \mathbf{p} - \mathbf{c}_{23}) = r_{12}^2 - r_{23}^2 \quad (7b)$$

$$2(\mathbf{c}_{23} - \mathbf{c}_{12})^T \mathbf{p} = r_{12}^2 - r_{23}^2 + \|\mathbf{c}_{23}\|_2^2 - \|\mathbf{c}_{12}\|_2^2 \quad (7c)$$

which is now linear in the unknown parameter \mathbf{p} .

3. NOISE ANALYSIS

Up to now the TOA noise has been assumed to be zero. In practice TOA measurements are corrupted by additive noise:

$$\hat{t}_i = t_i + n_i \quad (8)$$

where n_i is assumed to be an i.i.d. Gaussian random variable with zero mean and variance σ_n^2 . Noisy TOA measurements lead to noisy subtended angles:

$$\hat{\alpha}_{ij} = \alpha_{ij} + n_{ij} \quad (9)$$

where

$$n_{ij} = \omega(n_j - n_i) \quad (10)$$

is a zero-mean Gaussian random variable with variance $2\omega^2\sigma_n^2$. The n_{ij} are no longer independent due to common noise terms. The circle centre and radius values computed using noisy subtended angles become

$$\hat{\mathbf{c}}_{ij} = \mathbf{c}_{ij} + \mathbf{v}_{ij}, \quad \hat{r}_{ij} = r_{ij} + w_{ij} \quad (11)$$

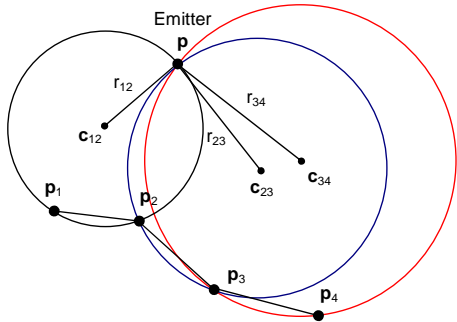


Figure 4: Scan-based emitter localization using four receivers.

where \mathbf{v}_{ij} and w_{ij} are additive circle centre and radius noise terms. For noisy parameters, (7c) can be re-written as

$$(\hat{\mathbf{c}}_{23} - \mathbf{v}_{23} - \hat{\mathbf{c}}_{12} + \mathbf{v}_{12})^T \mathbf{p} = \frac{1}{2} ((\hat{r}_{12} - w_{12})^2 - (\hat{r}_{23} - w_{23})^2 + \|\hat{\mathbf{c}}_{23} - \mathbf{v}_{23}\|_2^2 - \|\hat{\mathbf{c}}_{12} - \mathbf{v}_{12}\|_2^2) \quad (12a)$$

$$(\hat{\mathbf{c}}_{23} - \hat{\mathbf{c}}_{12})^T \mathbf{p} = \frac{1}{2} (\hat{r}_{12}^2 - \hat{r}_{23}^2 + \|\hat{\mathbf{c}}_{23}\|_2^2 - \|\hat{\mathbf{c}}_{12}\|_2^2) + \eta \quad (12b)$$

where η is the equation noise given by

$$\eta = (\mathbf{v}_{23} - \mathbf{v}_{12})^T \mathbf{p} - \hat{r}_{12} w_{12} + \hat{r}_{23} w_{23} + \hat{\mathbf{c}}_{12}^T \mathbf{v}_{12} - \hat{\mathbf{c}}_{23}^T \mathbf{v}_{23} + \frac{1}{2} (w_{12}^2 - w_{23}^2 - \|\mathbf{v}_{12}\|_2^2 + \|\mathbf{v}_{23}\|_2^2). \quad (13)$$

For sufficiently small TOA noise, the squared noise terms and products of noises can be ignored, yielding

$$\eta \approx (\mathbf{v}_{23} - \mathbf{v}_{12})^T \mathbf{p} - r_{12} w_{12} + r_{23} w_{23} + \mathbf{c}_{12}^T \mathbf{v}_{12} - \mathbf{c}_{23}^T \mathbf{v}_{23} \quad (14a)$$

$$\approx (\mathbf{p} - \mathbf{c}_{23})^T \mathbf{v}_{23} - (\mathbf{p} - \mathbf{c}_{12})^T \mathbf{v}_{12} + r_{23} w_{23} - r_{12} w_{12}. \quad (14b)$$

It is interesting to note that η is proportional to the radius of the circles.

4. LINEAR LEAST-SQUARES ESTIMATOR

A matrix equation linear in the unknown parameter \mathbf{p} can be formed by stacking (12b) for multiple TOA measurements at successive radar scans. This will tend to create an ill-conditioned least-squares (LS) problem unless receiver 2 moves very fast during radar scan periods, thereby creating a geometry where multiple circles intersect only in the vicinity of the emitter. Otherwise the locations of receiver 2 where TOA measurements were taken remain to be a possible LS solution in addition to the emitter. This makes the LS problem ill-conditioned, causing its solution to be extremely sensitive to noise.

The ill-conditioning or rank deficiency problem is avoided if four or more receivers are used for locating the emitter. The ghost emitters are also eliminated. A localization geometry for four receivers is shown in Fig. 4. In the remainder of this paper we will focus

on the case of four receivers with no lack of generality. Extension to more receivers is straightforward.

Using multiple subtended angle measurements $\hat{\alpha}_{12}(k)$, $\hat{\alpha}_{23}(k)$, $\hat{\alpha}_{34}(k)$, $k = 1, \dots, K$, collected by the four moving receivers, (12b) can be stacked to give

$$\underbrace{\begin{bmatrix} (\hat{\mathbf{c}}_{23}(1) - \hat{\mathbf{c}}_{12}(1))^T \\ (\hat{\mathbf{c}}_{34}(1) - \hat{\mathbf{c}}_{23}(1))^T \\ (\hat{\mathbf{c}}_{23}(2) - \hat{\mathbf{c}}_{12}(2))^T \\ (\hat{\mathbf{c}}_{34}(2) - \hat{\mathbf{c}}_{23}(2))^T \\ \vdots \\ (\hat{\mathbf{c}}_{23}(K) - \hat{\mathbf{c}}_{12}(K))^T \\ (\hat{\mathbf{c}}_{34}(K) - \hat{\mathbf{c}}_{23}(K))^T \end{bmatrix}}_{\mathbf{A}} \mathbf{p} = \underbrace{\begin{bmatrix} \hat{r}_{12}^2(1) - \hat{r}_{23}^2(1) + \|\hat{\mathbf{c}}_{23}(1)\|_2^2 - \|\hat{\mathbf{c}}_{12}(1)\|_2^2 \\ \hat{r}_{23}^2(1) - \hat{r}_{34}^2(1) + \|\hat{\mathbf{c}}_{34}(1)\|_2^2 - \|\hat{\mathbf{c}}_{23}(1)\|_2^2 \\ \hat{r}_{12}^2(2) - \hat{r}_{23}^2(2) + \|\hat{\mathbf{c}}_{23}(2)\|_2^2 - \|\hat{\mathbf{c}}_{12}(2)\|_2^2 \\ \hat{r}_{23}^2(2) - \hat{r}_{34}^2(2) + \|\hat{\mathbf{c}}_{34}(2)\|_2^2 - \|\hat{\mathbf{c}}_{23}(2)\|_2^2 \\ \vdots \\ \hat{r}_{12}^2(K) - \hat{r}_{23}^2(K) + \|\hat{\mathbf{c}}_{23}(K)\|_2^2 - \|\hat{\mathbf{c}}_{12}(K)\|_2^2 \\ \hat{r}_{23}^2(K) - \hat{r}_{34}^2(K) + \|\hat{\mathbf{c}}_{34}(K)\|_2^2 - \|\hat{\mathbf{c}}_{23}(K)\|_2^2 \end{bmatrix}}_{\mathbf{b}} + \underbrace{\begin{bmatrix} \eta_1(1) \\ \eta_2(1) \\ \eta_1(2) \\ \eta_2(2) \\ \vdots \\ \eta_1(K) \\ \eta_2(K) \end{bmatrix}}_{\boldsymbol{\eta}}. \quad (15)$$

An LS solution to the approximate matrix equation $\mathbf{A}\mathbf{p} \approx \mathbf{b}$ is given by

$$\hat{\mathbf{p}}_{\text{LS}} = (\mathbf{A}^T \mathbf{A})^{-1} \mathbf{A}^T \mathbf{b}. \quad (16)$$

Here \mathbf{A} is assumed to be full rank.

The correlation between the data matrix \mathbf{A} and the noise vector $\boldsymbol{\eta}$ makes the LS estimate biased. The bias of the LS estimate is

$$\boldsymbol{\beta} = E\{\hat{\mathbf{p}}_{\text{LS}} - \mathbf{p}\} = -E\{(\mathbf{A}^T \mathbf{A})^{-1} \mathbf{A}^T \boldsymbol{\eta}\}. \quad (17)$$

The large-sample bias may be approximated by $\boldsymbol{\beta} \approx -E\{\mathbf{A}^T \mathbf{A}\}^{-1} E\{\mathbf{A}^T \boldsymbol{\eta}\}$. Again the fact that $E\{\mathbf{A}^T \boldsymbol{\eta}\}$ does not vanish as $K \rightarrow \infty$ makes the LS estimator biased even if $K \rightarrow \infty$.

In long range situations, the noise covariance matrix $\mathbf{K} = E\{\boldsymbol{\eta}\boldsymbol{\eta}^T\}$ up to a scaling factor is approximately given by

$$\mathbf{K} \approx \begin{bmatrix} 1 & -1/2 & & & & & \mathbf{0} \\ -1/2 & 1 & -1/2 & & & & \\ & & \ddots & \ddots & \ddots & & \\ & & & \ddots & \ddots & \ddots & \\ & & & & \ddots & \ddots & \\ & & & & & -1/2 & 1 & -1/2 \\ \mathbf{0} & & & & & -1/2 & 1 & 1 \end{bmatrix}. \quad (18)$$

Because the TOA noise is i.i.d., the measurements at different radar scans are uncorrelated; i.e., $E\{\eta_i(k)\eta_j(l)\} = 0$ for $i, j \in \{1, 2\}$ and $k \neq l$. Assuming a long range geometry with almost identical circle radii, and uncorrelated $v_{ij}(k)$ and $w_{ij}(k)$, we have $E\{\eta_1^2(k)\} \approx E\{\eta_2^2(k)\}$ and $E\{\eta_1(k)\eta_2(k)\} \approx -0.5E\{\eta_1^2(k)\}$.

Using the noise covariance matrix \mathbf{K} given in (18) a weighted LS estimator can be formulated as follows:

$$\hat{\mathbf{p}}_{\text{WLS}} = (\mathbf{A}^T \mathbf{K}^{-1} \mathbf{A})^{-1} \mathbf{A}^T \mathbf{K}^{-1} \mathbf{b}. \quad (19)$$

5. MAXIMUM LIKELIHOOD ESTIMATOR

The conditional joint probability density function (pdf) of the subtended angle measurements $\hat{\alpha}_{12}(k)$, $\hat{\alpha}_{23}(k)$, $\hat{\alpha}_{34}(k)$ given an emitter location \mathbf{x} is

$$f(\hat{\boldsymbol{\alpha}}|\mathbf{x}) = \frac{1}{(2\pi)^K |\boldsymbol{\Sigma}|^{1/2}} \exp\left\{-\frac{1}{2}(\hat{\boldsymbol{\alpha}} - \boldsymbol{\alpha}(\mathbf{x}))^T \boldsymbol{\Sigma}^{-1} \times (\hat{\boldsymbol{\alpha}} - \boldsymbol{\alpha}(\mathbf{x}))\right\} \quad (20)$$

where $\hat{\boldsymbol{\alpha}}$ is the vector of measured angles at multiple radar scans

$$\hat{\boldsymbol{\alpha}} = [\hat{\alpha}_{12}(1), \hat{\alpha}_{23}(1), \hat{\alpha}_{34}(1), \dots, \hat{\alpha}_{12}(K), \hat{\alpha}_{23}(K), \hat{\alpha}_{34}(K)]^T$$

$\boldsymbol{\alpha}(\mathbf{x})$ is the subtended angles vector as a function of the emitter location \mathbf{x}

$$\boldsymbol{\alpha}(\mathbf{x}) = \begin{bmatrix} \cos^{-1} \frac{\|\mathbf{p}_1(1) - \mathbf{x}\|_2^2 + \|\mathbf{p}_2(1) - \mathbf{x}\|_2^2 - \|\mathbf{p}_2(1) - \mathbf{p}_1(1)\|_2^2}{2\|\mathbf{p}_1(1) - \mathbf{x}\|_2 \|\mathbf{p}_2(1) - \mathbf{x}\|_2} \\ \cos^{-1} \frac{\|\mathbf{p}_2(1) - \mathbf{x}\|_2^2 + \|\mathbf{p}_3(1) - \mathbf{x}\|_2^2 - \|\mathbf{p}_3(1) - \mathbf{p}_2(1)\|_2^2}{2\|\mathbf{p}_2(1) - \mathbf{x}\|_2 \|\mathbf{p}_3(1) - \mathbf{x}\|_2} \\ \cos^{-1} \frac{\|\mathbf{p}_3(1) - \mathbf{x}\|_2^2 + \|\mathbf{p}_4(1) - \mathbf{x}\|_2^2 - \|\mathbf{p}_4(1) - \mathbf{p}_3(1)\|_2^2}{2\|\mathbf{p}_3(1) - \mathbf{x}\|_2 \|\mathbf{p}_4(1) - \mathbf{x}\|_2} \\ \vdots \\ \cos^{-1} \frac{\|\mathbf{p}_1(K) - \mathbf{x}\|_2^2 + \|\mathbf{p}_2(K) - \mathbf{x}\|_2^2 - \|\mathbf{p}_2(K) - \mathbf{p}_1(K)\|_2^2}{2\|\mathbf{p}_1(K) - \mathbf{x}\|_2 \|\mathbf{p}_2(K) - \mathbf{x}\|_2} \\ \cos^{-1} \frac{\|\mathbf{p}_2(K) - \mathbf{x}\|_2^2 + \|\mathbf{p}_3(K) - \mathbf{x}\|_2^2 - \|\mathbf{p}_3(K) - \mathbf{p}_2(K)\|_2^2}{2\|\mathbf{p}_2(K) - \mathbf{x}\|_2 \|\mathbf{p}_3(K) - \mathbf{x}\|_2} \\ \cos^{-1} \frac{\|\mathbf{p}_3(K) - \mathbf{x}\|_2^2 + \|\mathbf{p}_4(K) - \mathbf{x}\|_2^2 - \|\mathbf{p}_4(K) - \mathbf{p}_3(K)\|_2^2}{2\|\mathbf{p}_3(K) - \mathbf{x}\|_2 \|\mathbf{p}_4(K) - \mathbf{x}\|_2} \end{bmatrix} \quad (21)$$

and $\boldsymbol{\Sigma}$ is the covariance matrix of subtended angle measurements

$$\boldsymbol{\Sigma} = 2\omega^2 \sigma_n^2 \begin{bmatrix} 1 & -1/2 & & & & & & & & \mathbf{0} \\ -1/2 & 1 & -1/2 & & & & & & & \\ & & \ddots & \ddots & \ddots & & & & & \\ & & & \ddots & \ddots & \ddots & & & & \\ & & & & \ddots & \ddots & \ddots & & & \\ & & & & & -1/2 & 1 & -1/2 & & \\ \mathbf{0} & & & & & & -1/2 & 1 & -1/2 & \\ & & & & & & & & & 1 \end{bmatrix} \quad (22)$$

Maximizing the log-likelihood function over \mathbf{x} gives the ML estimate $\hat{\mathbf{p}}_{\text{ML}} = \arg \min_{\mathbf{x}} J_{\text{ML}}(\mathbf{x})$ where

$$J_{\text{ML}}(\mathbf{x}) = \mathbf{e}^T(\mathbf{x}) \boldsymbol{\Sigma}^{-1} \mathbf{e}(\mathbf{x}), \quad \mathbf{e}(\mathbf{x}) = \hat{\boldsymbol{\alpha}} - \boldsymbol{\alpha}(\mathbf{x}). \quad (23)$$

The ML optimization problem does not have a closed-form solution. Thus an iterative search algorithm, such as the Gauss-Newton (GN) algorithm [4],

is required to find a numerical solution. The GN algorithm has the following form:

$$\mathbf{p}(i+1) = \mathbf{p}(i) - (\mathbf{J}^T(i) \boldsymbol{\Sigma}^{-1} \mathbf{J}(i))^{-1} \mathbf{J}^T(i) \boldsymbol{\Sigma}^{-1} \mathbf{e}(\mathbf{p}(i)), \quad i = 0, 1, \dots \quad (24)$$

where $\mathbf{J}(i)$ is the Jacobian matrix of $\mathbf{e}(\mathbf{x})$ with respect to \mathbf{x} evaluated at $\mathbf{x} = \mathbf{p}(i)$:

$$\mathbf{J}(i) = \begin{bmatrix} \frac{\partial e_{12}(1)}{\partial \mathbf{x}} & \frac{\partial e_{23}(1)}{\partial \mathbf{x}} & \frac{\partial e_{34}(1)}{\partial \mathbf{x}} \\ \dots & \frac{\partial e_{12}(K)}{\partial \mathbf{x}} & \frac{\partial e_{23}(K)}{\partial \mathbf{x}} & \frac{\partial e_{34}(K)}{\partial \mathbf{x}} \end{bmatrix} \Bigg|_{\mathbf{x}=\mathbf{p}(i)} \quad (25)$$

with $\mathbf{e}(\mathbf{x}) = [e_{12}(1), e_{23}(1), e_{34}(1), \dots, e_{12}(K), e_{23}(K), e_{34}(K)]^T$.

The GN algorithm is identical to the Taylor series method [5]. The initial guess for the GN algorithm, $\mathbf{p}(0)$, must be close to the ML estimate to avoid undesirable divergence problems. An initial guess may be obtained from the geometric solution given in (5) after replacing \mathbf{c}_{ij} and r_{ij} with their noisy counterparts $\hat{\mathbf{c}}_{ij}(k)$ and $\hat{r}_{ij}(k)$, respectively, at one of the angle measurements, say, $k = 1$. A better alternative is to use the WLS estimate. Other search techniques such as the Nelder-Mead simplex method [6] can also be employed to find the ML estimate.

6. SIMULATION STUDIES

In the simulations the radar to be located is assumed to be placed at $\mathbf{p} = [10, 20]^T$ km in two-dimensional Cartesian coordinates. The sweep rate of the radar is $\omega = \pi$ rad/s. The speed of propagation for emitted radar pulses is assumed to be $c = 3 \times 10^5$ km/s. The four moving receivers collect $K = 10$ TOA measurements roughly every 2 s which is the rotation period for the radar. The initial locations of the receivers are $\mathbf{p}_1(1) = [-10, 5]^T$, $\mathbf{p}_2(1) = [2, -2]^T$, $\mathbf{p}_3(1) = [10, 0]^T$ and $\mathbf{p}_4(1) = [20, 2]^T$ km. The receivers are assumed to move with constant velocity $[-.01, .04]^T$, $[.02, .03]^T$, $[.01, .04]^T$ and $[-.01, .04]^T$ km/s.

The ML estimator was implemented using the Nelder-Mead simplex method with an initial guess obtained from the WLS estimate. The bias and mean-square error (MSE) performance of the LS, WLS and ML estimators was simulated using 1000 Monte Carlo simulation runs. The circles corresponding to a realization of $K = 10$ noisy TOA measurements at $\sigma_n = 1$ ms are plotted in Fig. 5. Fig. 6 shows the 68% error ellipses (confidence regions) for LS and WLS estimates. The WLS estimate exhibits a significant bias reduction in comparison with the LS estimate. The bias and MSE results for the LS, WLS and ML estimates are shown in Figs. 7 and 8, respectively, for a range of TOA noise standard deviation. Fig. 8 also plots the Cramer-Rao lower bound (CRLB). The simulations reveal the benefit of employing a weighting matrix in the LS estimator in terms of bias and MSE reduction. The best bias and MSE performance is obtained from the ML estimator.

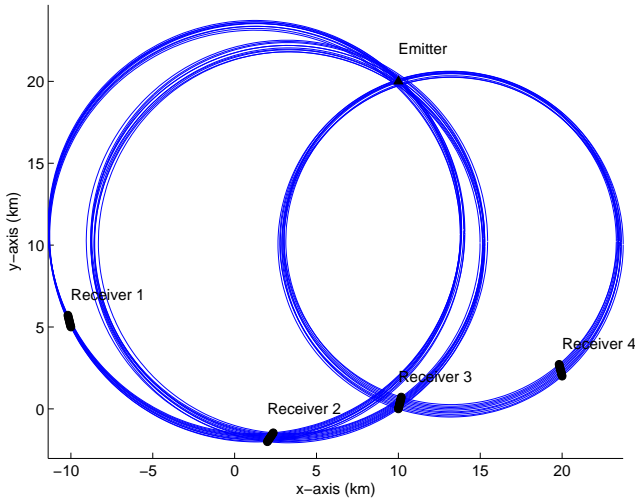


Figure 5: The circles for a realization of $K = 10$ sets of TOA measurements collected at four moving receivers. The TOA noise standard deviation is $\sigma_n = 1$ ms.

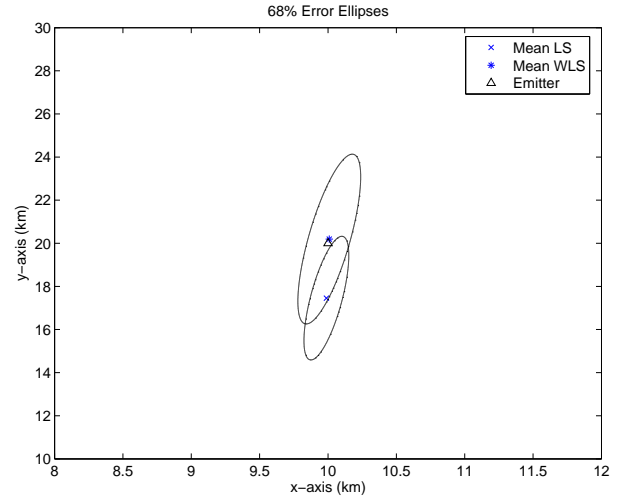


Figure 6: 68% error ellipses for LS and WLS estimates at $\sigma_n = 1$ ms. Note the improved bias performance for the WLS estimate.

In terms of computational complexity, the ML estimator is the most demanding algorithm while the complexities of LS and WLS are comparable.

7. CONCLUSION

WLS and ML estimators were developed for scan-based emitter localization using multiple scan measurements. Significant performance improvement for these algorithms was demonstrated by way of computer simulations. Other bias reduction techniques such as instrumental variables and total least squares will be considered in future work.

REFERENCES

- [1] H. Hmam, "Scan-based emitter passive localization," *IEEE Trans. on Aerospace and Electronic Systems*, accepted.
- [2] C. D. McGillem and T. S. Rappaport, "A beacon navigation method for autonomous vehicles," *IEEE Trans. on Vehicular Technology*, vol. 38, no. 3, pp. 132–139, August 1989.
- [3] I. Shimshoni, "On mobile robot localization from landmark bearings," *IEEE Trans. Robotics and Automation*, vol. 18, no. 6, pp. 971–976, December 2002.
- [4] L. Ljung and T. Söderström, *Theory and Practice of Recursive Identification*. Cambridge, MA: MIT Press, 1983.
- [5] W. H. Foy, "Position-location solutions by Taylor-series estimation," *IEEE Trans. on Aerospace and Electronic Systems*, vol. 12, no. 2, pp. 187–194, March 1976.
- [6] J. A. Nelder and R. Mead, "A simplex method for function minimization," *Computer Journal*, vol. 7, pp. 308–313, 1965.

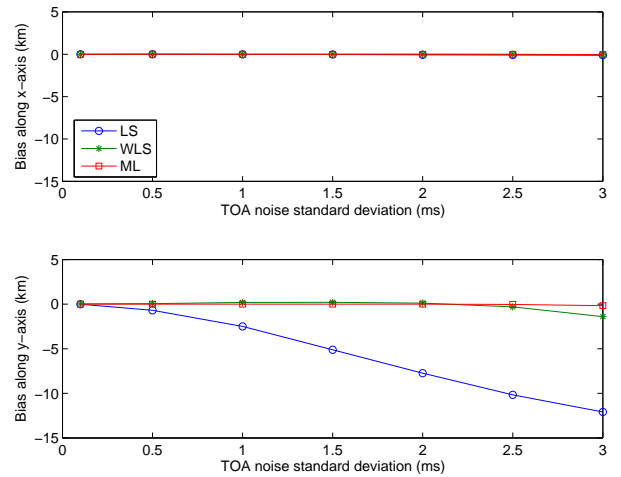


Figure 7: Bias of the LS, WLS and ML estimates as a function of TOA noise standard deviation.

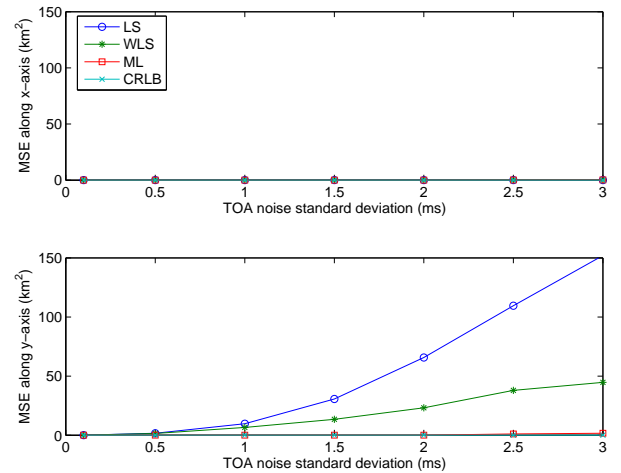


Figure 8: MSE of the LS, WLS and ML estimates as a function of TOA noise standard deviation.